Revista Mexicana de Astronomía y Astrofísica, **33**, 173–185 (1997)

APPLICATIONS OF POLYNOMIAL TRANSFORMS IN ASTRONOMICAL IMAGE RESTORATION AND DECONVOLUTION

S. Venegas-Martínez[1], B. Escalante-Ramírez[1], and J. A. García-Barreto[2]

Received 1996 June 14; accepted 1997 September 8

RESUMEN

El presente trabajo muestra algunas aplicaciones de la teoría de las transformaciones polinomiales al procesamiento digital de imágenes astronómicas (reducción de ruido, perfilación y codificación). Para interpretar datos a partir de una imagen astronómica, es necesario obtener información explícita importante. Esto usualmente implica la determinación de las relaciones entre las intensidades de los pixeles, lo cual requiere alguna forma de procesamiento local de los datos en toda la imagen. Este trabajo se enfoca en el esquema basado para el procesamiento local de la información en imágenes astronómicas, llamado transformada de Hermite. Esta transformada es un modelo de representación que analiza una imagen expandiéndola localmente en una suma ponderada de polinomios ortogonales. Las aplicaciones que proponemos se desarrollan sobre estructuras piramidales. El propósito es analizar imágenes astronómicas en longitudes de onda del visible, a diferentes escalas espaciales. Este método se ha aplicado a imágenes ópticas astronómicas obtenidas en el telescopio de 2.12-m en el Observatorio Astronómico Nacional en San Pedro Mártir, México.

ABSTRACT

Based on the polynomial transform theory we show applications for noise reduction, deconvolution and coding in astronomical images. The proper interpretation of an astronomical image, requires to obtain relevant information from the structures contained in it. This procedure requires to process the data locally. For our applications, it is required that the image data, which are given as an array of intensity values, be interpreted into meaningful patterns. For this purpose, we use the Hermite transform. This transform is an image representation model that analyzes an image by locally expanding it into a weighted sum of orthogonal polynomials. The applications that we propose are developed on pyramidal structures. Their purpose is to analyze optical astronomical images at different spatial scales.

Key words: **TECHNIQUES – IMAGE PROCESSING**

1. INTRODUCTION

A problem in CCD astronomical images is the masking of low-contrast features by presence of noise. The problem arises since many of the more important astronomical features are often composed of faint intensity changes that do not conform sharp contours. According to the Scale-Space theory (Koenderink 1984), these objects are best represented at low-spatial resolutions. High intensity contours might exist in astronomical images, for example in galaxy nuclei which are unresolved from earth based telescopes. An efficient noise reduction algorithm must therefore, be able to process adaptively an image at multiple spatial resolutions.

A second problem in astronomical imaging is the combined effect of the atmosphere, telescope and camera limitations that results in a convolved point-spread-function that seriously degrades the image

[1] División de Estudios de Posgrado, Fac. de Ingeniería, Universidad Nacional Autónoma de México.

[2] Instituto de Astronomía, Universidad Nacional Autónoma de México.

quality. For the sake of simplicity, we will consider this PSF as spatial invariant (the experimental results of the image processing algorithms presented in this paper suggest that this assumption does not imply serious errors). Relevant enhancement processing techniques should therefore, deal with deconvolving methods in order to obtain sharper images. If an image includes noise, however, the deconvolution technique should be able to restore the best image, i.e., it should deconvolve the locations of the image where only relevant information (contours at different resolutions) is present.

Both noise reduction and image deconvolution must be based on an image representation model that incorporates multiresolution and adaptability to the image contents. Several efforts towards this direction have appeared in the last years with applications in optical astronomy. An example of this approach was developed by Richter et al. (1991) by means of a resolution-adaptive filtering technique based on approximating the Karhunen-Loeve transform in non-overlapping blocks within the image. This approximation results in the so-called H-transform (after Haar 1910) and has become a popular technique in astronomical imaging. A known disadvantage, however, of any non-overlapping block-processing such as the H-transform and the Discrete Cosine transform, which is also a local approximation of the Karhunen-Loeve transform, is the introduction of blocking effects. The technique presented by them overcomes this problem by low-pass filtering the resulting image. This, of course, blurs the final image, as will be shown in § 6.

In order to avoid blocking effects, images should be analyzed on a local basis by means of overlapping analysis windows. For the analysis to be complete, analysis at different spatial resolutions should be applied. This strategy is strongly supported by the Scale Space theory. Based on this theory, a series of multiresolution image models have emerged with applications in astronomy. This is the case of the work by Starck, Murtagh, & Bijaoui (1995), who presented general principles for designing processing techniques for restoration, detection and compression with applications in astronomy, based on wavelet transforms. More specific applications can be found in Bijaoui & Rué (1995), where a wavelet-based model for astronomical object detection is presented. Object features are extracted from a multiscale image restoration algorithm. Starck et al. (1996) proposed an algorithm for astronomical image compression based on a multiscale morphological transform. Their algorithm achieves high compression rates by supressing noise in an image. We show in this paper similar applications.

We present specific algorithms for the restoration, deconvolution and coding of astronomical images based on the polynomial transform. This transform is based on analyzing the image by means of overlapping windows, and representing the local image content as a sum of weighted polynomials that are orthogonal with respect to the analysis window. In the case of a Gaussian analysis window, the orthogonal polynomials correspond to the Hermite functions (Szegö 1959). The operators used to obtain the weighting polynomial coefficients can be shown to be derivatives of Gaussian functions. These operators have been long used in computer vision in order to efficiently detect primitive image patterns such as edges and lines, and have been identified as good models of the response of retinal and cortical cells (Young 1985). In the specific case of the first-order derivative of a Gaussian, Canny (1983, 1986) showed that this operator is close to the statistical optimal edge detector. The scheme proposed in this paper performs analysis with the polynomial transform at different resolutions, i.e., using analysis windows of different sizes. This will allow us to detect large and smooth astronomical structures (e.g., clouds), as well as sharp intensity transitions.

In this paper we show processing results of the image enhancement techniques that we propose. We present a comparison with other popular techniques used in astronomy, namely median filter and H-transform filter. A sample of the application of these techniques in astronomical research is appreciated in the Hα spatial distribution in barred galaxies by García-Barreto et al. (1996). The images presented in this paper have been processed with the Polynomial transform methods.

In order to show the potential of the polynomial transform as a general tool for astronomical image processing, we present in addition, deconvolution and coding in a multiresolution analysis-synthesis structure. Coding in this case is implemented by a prediction scheme that preserves only relevant information (structures) while throwing away noise (Venegas et al. 1995).

2. THE POLYNOMIAL TRANSFORM

In order to analyze an image on a local basis, the image $L(x, y)$ is multiplied by a window function $V(x, y)$. This windowing takes place at several positions (p, q) over the entire input image, comprising a sampling lattice S. By repetition of the window function over the sampling lattice, a periodic weighting function $W(x, y)$ is defined as

$$W(x, y) = \sum_{(p,q)\varepsilon S} V(x - p, y - q) \quad . \qquad (1)$$

Provided $W(x, y)$ is nonzero, for all (x, y), we obtain

$$L(x, y) = \frac{1}{W(x, y)} \sum_{(p,q)\varepsilon S} L(x, y)\, V(x-p, y-q) \quad . \quad (2)$$

Within every window $V(x-p, y-q)$, the image is described by a weighted sum of polynomials $G_{m,n-m}(x,y)$ of degree m in x, and $n-m$ in y. We use polynomials that are orthogonal with respect to the window function (Szegö 1959), i.e.,

$$\int_{-\infty}^{+\infty}\int_{-\infty}^{+\infty} V^2(x,y) \; G_{m,n-m}(x,y)G_{l,k-l}(x,y)dx\,dy = \delta_{nk}\,\delta_{ml} \quad , \quad (3)$$

for $n,k = 0,\ldots,\infty$, $m = 0,\ldots,n$ and $l = 0,\ldots,k$, where $\delta_{n,k}$ denotes the Kroenecker function. When a Gaussian window is used, for instance, the Hermite polynomials are chosen for the expansion.

The polynomial expansion within the window $V(x-p, y-q)$ is described by

$$V(x-p,y-q)\left[L(x,y) - \sum_{n=0}^{\infty}\sum_{m=0}^{n} L_{m,n-m}(p,q)\cdot G_{m,n-m}(x-p,y-q)\right] = 0 \quad . \quad (4)$$

By multiplying eq. 4 by $V(x-p,y-q)\,G_{l,k-l}(x-p,y-q)$, and applying the orthogonality condition of eq. 3, we observe that the polynomial coefficients $L_{m,n-m}(p,q)$ belonging to the polynomials $G_{m,n-m}(x-p,y-q)$, for all positions $(p,q)\,\varepsilon S$ of the window function $V(x-p,y-q)$, are derived by convolving the input image $L(x,y)$ with a filter

$$D_{m,n-m}(x,y) = G_{m,n-m}(-x,-y)\,V^2(-x,-y) \quad , \quad (5)$$

and selecting the outputs

$$L_{m,n-m}(p,q) = \int_{-\infty}^{+\infty}\int_{-\infty}^{+\infty} L(x,y)\,D_{m,n-m}(p-x,q-y)\,dx\,dy \quad , \quad (6)$$

at the positions (p,q) in the sampling lattice S, for $m = 0,\ldots,n$ and $n = 0,\ldots,\infty$. In practice, the maximum order of the polynomial expansion will be limited to a finite number N. Figure 1 shows a polynomial expansion of the optical image of galaxy M51 for $N = 4$. The M51 optical image was taken from the examples given in the IRAF software package.

The mapping from the input signal to the weights of the polynomials, henceforth referred to as the polynomial coefficients, is called a forward polynomial transform.

The resynthesized image $\hat{L}(x,y)$ is obtained by the interpolation process of the inverse transform, i.e., substitution of eq. 4 in eq. 2 results in

$$\hat{L}(x,y) = \sum_{n=0}^{N}\sum_{m=0}^{n}\sum_{(p,q)\varepsilon S} L_{m,n-m}(p,q)\,P_{m,n-m}(x-p,y-q) \quad , \quad (7)$$

where the interpolation functions are defined by

$$P_{m,n-m}(x,y) = G_{m,n-m}(x,y)\,V(x,y)/W(x,y) \quad , \quad (8)$$

for $m = 0,\ldots,n$ and $n = 0,\ldots,N$. The only condition for the existence of the polynomial transform is that this weighting function be different from zero for all coordinates (x,y).

There are a number of parameters that have to be chosen in the definition of a polynomial transform. First, the type of window function must be selected. The Gaussian window is a good choice. It is separable and is rotationally symmetric. The Gaussian window and its derivatives, which are the operators of the polynomial transform in this case, provide an adequate model for the receptive fields in the visual system (Young 1985). The orthogonal polynomials associated with the Gaussian window are the Hermite polynomials (Szegö 1959). The resulting polynomial transform is called the Hermite transform, and it can be shown (Martens 1990) that the analysis filters in this case are given by

$$D_{m,n-m}(x,y;\sigma) = \frac{1}{\sqrt{2^n m!(n-m)!}}\frac{1}{\pi\sigma^2} H_m(x/\sigma)\,H_{n-m}(y/\sigma)\,\exp\left[\frac{-(x^2+y^2)}{\sigma^2}\right] \quad , \quad (9)$$

where $H_n(x)$ is the Hermite polynomial of degree n in x. It is interesting to note that the functions $D_{m,n-m}(x,y;\sigma)$ are equal to derivatives of a Gaussian (Martens 1990). Gaussian derivatives have proven to be useful for detecting local features in images such as contours.

For a discrete implementation of the polynomial transform, it is well known that the discrete counterpart of a Gaussian window is the binomial window (Martens 1990), i.e.,

$$V^2(x) = \frac{1}{2^M}C_M^x \quad , \quad (10)$$

for $x = 0,\ldots,M$, where M is the order of the binomial window. The orthogonal polynomials associated to the binomial window are the Krawtchouck polynomials

$$G_n(x) = \frac{1}{\sqrt{C_M^n}}\sum_{k=0}^{n}(-1)^{n-k}C_{M-x}^{n-k}C_x^k \quad , \quad (11)$$

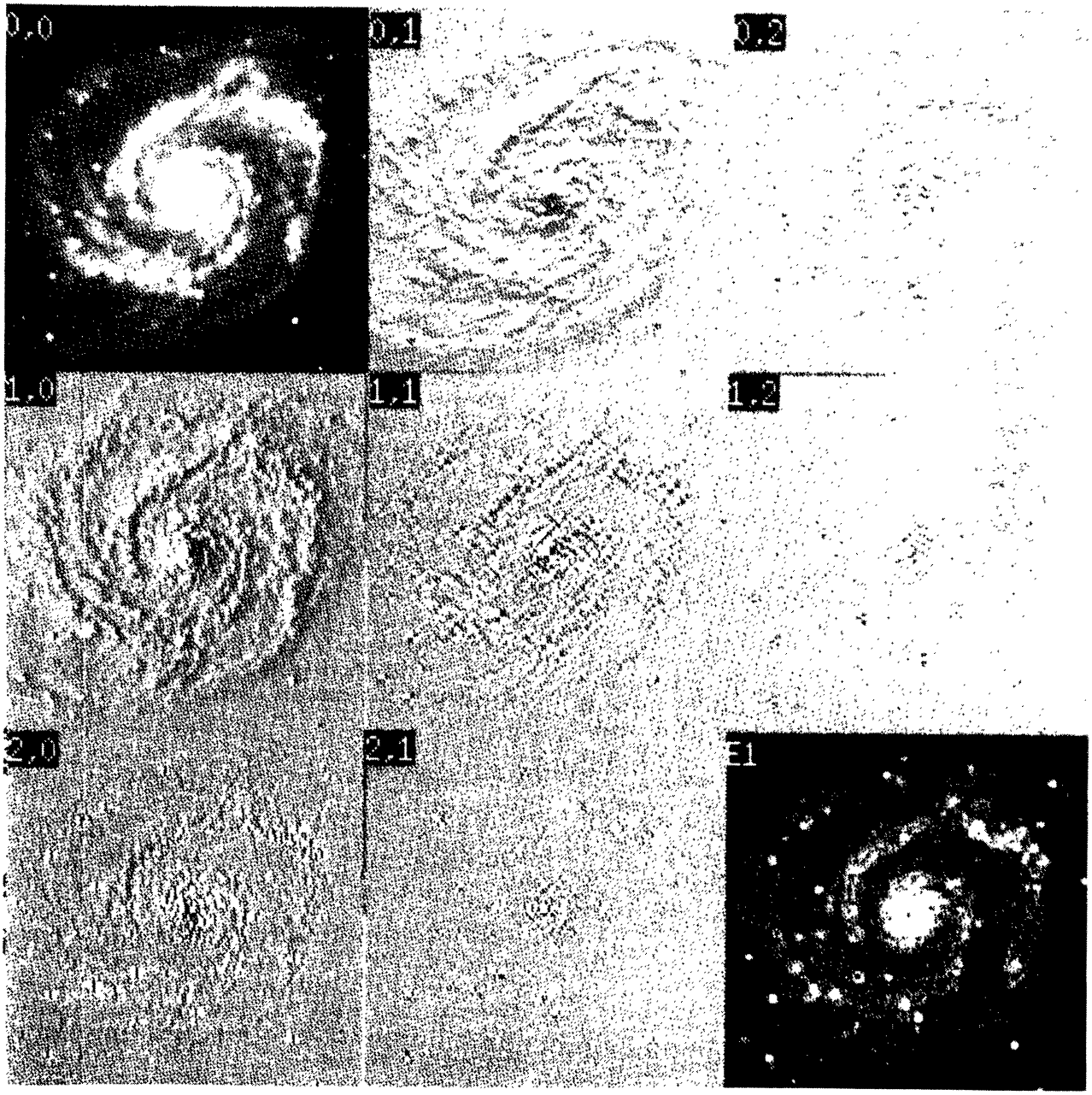

Fig. 1. An example of a single-scale polynomial-transform expansion of the galaxy M51 is shown. The expansion was obtained with a binomial analysis window of order 2. Each subimage represents the polynomial coefficients $L_{n,m}$, where the order of the polynomial n, m is indicated at the top of each frame. Subimage E_1 corresponds to the energy of the first order coefficients, i.e., $L_{0,1}$ and $L_{1,0}$.

for $n = 0, \ldots, M$. For large values of M, the binomial window approaches the Gaussian window, i.e.,

$$\lim_{M\to\infty} \frac{1}{2^M} C_M^{x+M/2} = \frac{1}{\sqrt{\pi}\sqrt{M/2}} \exp\left[-\left(\frac{x}{\sqrt{M/2}}\right)^2\right] , \quad (12)$$

for $x = -(M/2), \ldots, M/2$. A similar process turns a Krawtchouck polynomial into a Hermite polynomial

$$\lim_{M\to\infty} G_n\left(x + \frac{M}{2}\right) = \frac{1}{\sqrt{2^n n!}} H_n\left(\frac{x}{\sqrt{M/2}}\right) . \quad (13)$$

Since the binomial window is compactly supported

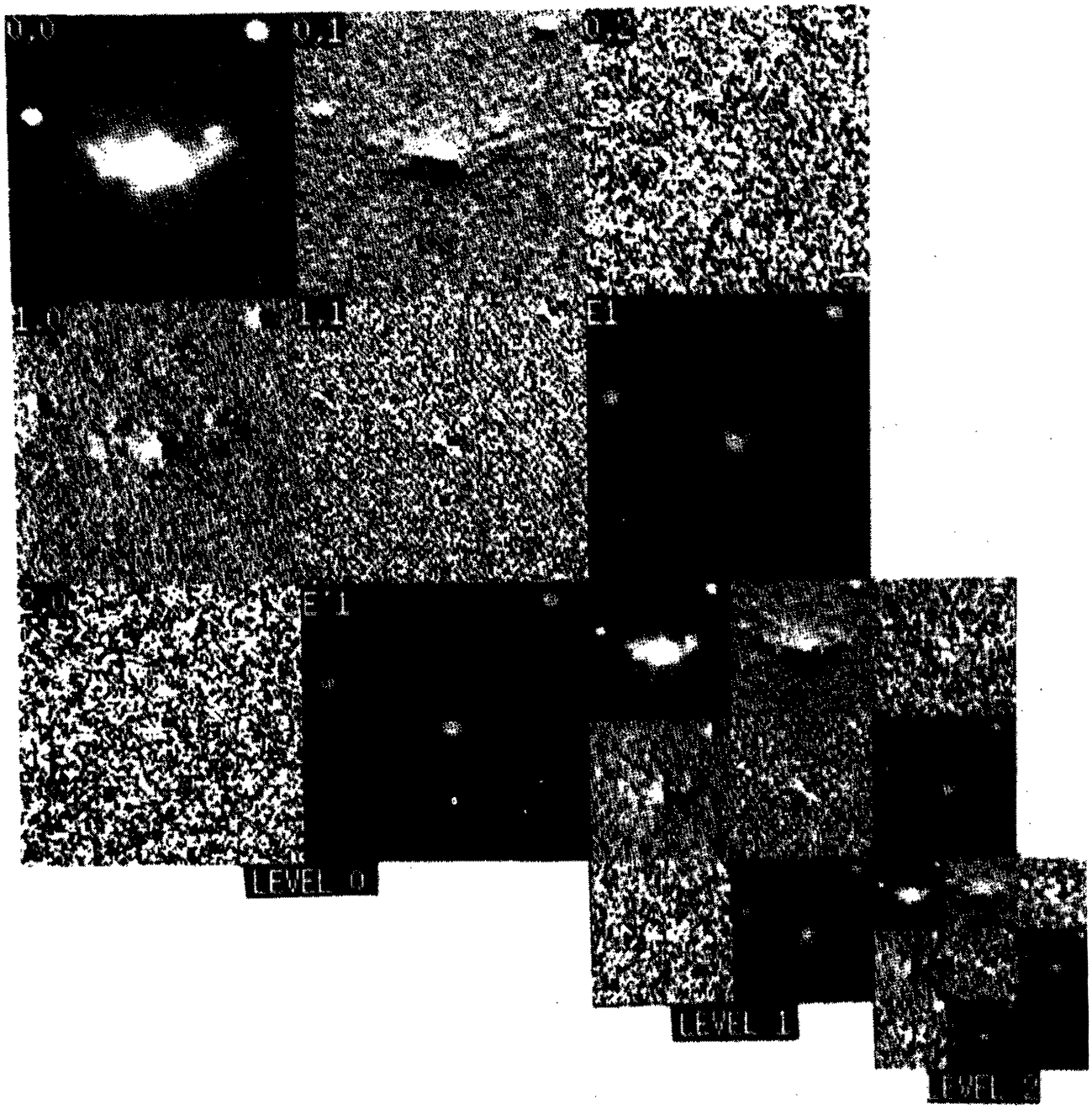

Fig. 2. A three-resolution polynomial-transform expansion of an astronomical image is presented. Level 0 corresponds to the highest resolution, obtained with a binomial window of order 2. Resolution levels 1 and 2 were obtained with equivalent window orders of 8 and 32 respectively.

(length $M+1$), the maximum order of the polynomial expansion is M, and the resynthesized digital image $\hat{L}(x, y)$ is identical to the original $L(x, y)$.

The second important parameter to be set is the size of the window function, also referred to as the spatial scale of the polynomial transform. In our case, we use a pyramidal coding structure, i.e., a multiresolution implementation of the polynomial transform, this being equivalent to selecting multiple window sizes, starting with a small size for the first pyramid level. See Figure 2 for an example of a multiresolution polynomial expansion of the optical image of galaxy NGC 1275. This image was taken at the 2.12-m telescope at the Observatorio Astronómico Nacional at San Pedro Mártir, México with an I filter and a CCD camera and kindly provided by Carrillo (1995).

3. METHOD OF DECONVOLUTION

Deconvolution is important in astronomical images, since the spatial limited resolution of the acquisition elements (lenses, electronics, etc.), combined with the atmosphere optical effects result in a convolved PSF. In this paper we will provide a solution based on the Hermite Transform for the case that the PSF be Gaussian-shaped. Although real PSFs often do not obey this model, they can be fairly approximated to the Gaussian. Many, if not all, optical images have noise features in addition to the astronomical objects. Some current deconvolution algorithms do not consider simultaneously noise reduction and deconvolution in the processing of the images. We will effectively tackle this problem in § 5 by proposing an adaptive deconvolution algorithm that adapts the deconvolution degree to the image content. In this section we will limit ourselves to present the deconvolution principle that will be used in § 5.

Let us suppose that the function $G(x,y)$ represents an image degradation system, such as the PSF of a telescope. Then, the image $L(x,y)$ convolved with the function $G(x,y)$, is

$$L'(x,y) = L(x,y) * G(x,y) \quad . \tag{14}$$

The polynomial coefficients of the convolved image are then given by

$$\begin{aligned} L'_{m,n-m}(p,q) &= [(L(x,y)*G(x,y))*D_{m,n-m}(x,y)]_{(p,q)} \\ &= [L(x,y) * (G(x,y) * D_{m,n-m}(x,y))]_{(p,q)} \\ &= [L(x,y) * D'_{m,n-m}(x,y)]_{(p,q)} \quad , \end{aligned} \tag{15}$$

where

$$D'_{m,n-m}(x,y) = D_{m,n-m}(x,y) * G(x,y) \tag{16}$$

is the convolved analysis filter. In other words, the polynomial coefficients of an image blurred by a function $G(x,y)$, obtained with the analysis filters $D_{m,n-m}(x,y)$, are the same as the polynomial coefficients of the unblurred image obtained with the blurred analysis filters $D'_{m,n-m}(x,y)$.

Having the Hermite transform and if the $G(x,y)$ is a Gaussian convolving function with standard deviation σ_B, as is our case, then Kayargadde & Martens (1994) showed that

$$D'_{m,n-m}(x,y;\sigma) = \left(\frac{1}{\sqrt{1+(\sigma_B/\sigma)^2}}\right)^n D_{m,n-m}(x,y;\sigma\sqrt{1+(\sigma_B/\sigma)^2}) \quad . \tag{17}$$

It follows from this equation and from eq. 6, that the Hermite coefficients of the convolved signal $L'_{m,n-m}(p,q;\sigma)$ are given by

$$L'_{m,n-m}(p,q;\sigma) = \left(\frac{1}{\sqrt{1+(\sigma_B/\sigma)^2}}\right)^n L_{m,n-m}(p,q;\sigma\sqrt{1+(\sigma_B/\sigma)^2}) \quad . \tag{18}$$

This means that the Hermite coefficients of an image after convolving with a Gaussian function with spread σ_B, obtained with an analysis window of spread σ, are the same as the Hermite coefficients of an image obtained with a window of spread

$$\sigma' = \sigma\sqrt{1+(\sigma_B/\sigma)^2} \quad , \tag{19}$$

weighted by a factor $(1/\sqrt{1+(\sigma_B/\sigma)^2})^n$.

This conclusion immediately suggests a deconvolution algorithm. In order to recover the original image $L(x,y)$ from the polynomial coefficients of the convolved image $L'(x,y)$ the synthesis filters of eq. 8 have to be designed using an analysis window $V(x,y;\sigma')$, where σ' is given by eq. 19, and weighted by a factor $(\sqrt{1+(\sigma_B/\sigma)^2})^n$. Figure 3 illustrates this deconvolution process for the image of the galaxy M51 .

4. MULTIRESOLUTION NOISE-REDUCTION SCHEME

The basic problem in noise reduction leads to a compromise between smoothing noisy regions and preserving the sharpness of important image features. We tackle the noise-reduction problem by explicitly making a systematic distinction between edges and homogeneous regions so that the smoothing process adapts itself to the image content. In order to achieve this distinction, we have to analyze locally the image. As shown in § 2, this analysis is achieved by multiplying the image with overlapping analysis windows. There are a number of conflicting demands that have an influence on the choice of the window function. The window size is limited, at the low and the high end. If the window size is less than the correlation length of the noise, smoothing the noise within a window has little or no effect. Increasing the window size beyond the point where the smoothed noise reaches the visibility threshold makes no sense either. The theoretical argument for increasing the window size is that it allows the noise spread to be reduced. Another reason is that it is more reliable to make a decision between edges and noise if the window size is large. A disadvantage of increasing the window size is that the number of coefficients needed to adequately reconstruct the image grows with the window size, resulting in a high computational cost of the algorithm. A more serious

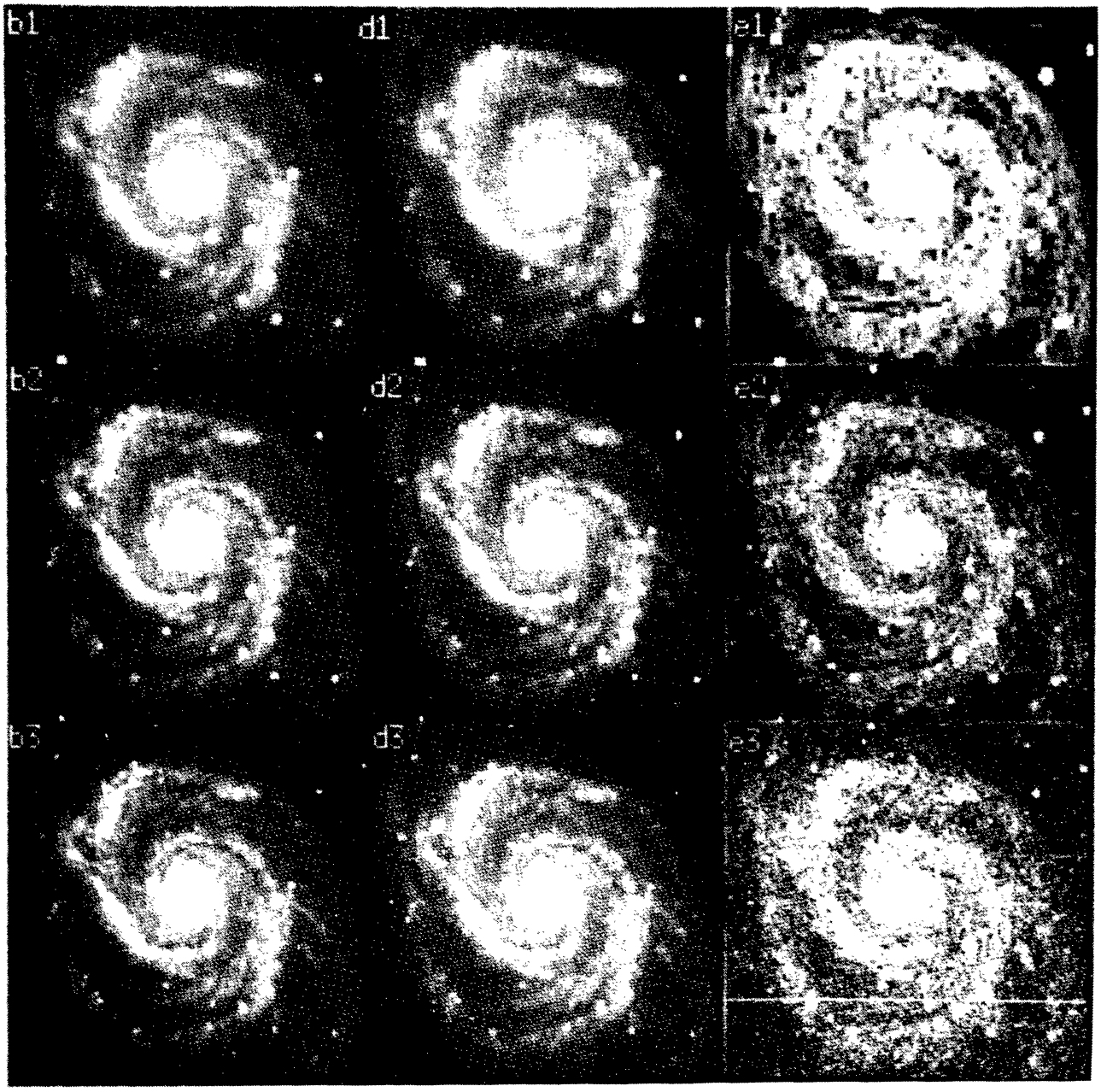

Fig. 3. An example of deconvolving with galaxy M51 is illustrated. $b1$, $b2$, and $b3$ represent images obtained by successively convolving the image with a Gaussian filter with $\sigma = 2$. $d1$, $d2$, and $d3$ present a successive sequence of deconvolved mages. $e1$, $e2$, and $e3$ represent the energy of the first-order polynomial coefficients at each resolution level.

disadvantage is that the presence of an edge inhibits the noise smoothing in its neighborhood. Hence, a band of unreduced noise occurs along the edges. In order to reduce the width of the noise band, it is necessary to reduce the window size, especially for high-contrast edges. This is possible because high-contrast edges can be reliably detected with small windows.

We can conclude that an optimum noise reduction is not possible with a single window function. It is preferable that the size of the window function be decreased for increasing edge amplitudes and decreasing distances from the edge. A well known technique for implementing such a variable-window processing is to use pyramidal structures (Burt & Adelson 1983).

4.1. Signal Detection

As already pointed out, one of the advantages of the Hermite transform over other transform-based processing methods, is the fact that the operators used to obtain the polynomial expansion are derivatives of a Gaussian. The properties of these operators as efficient primitive-structures detectors are well known in the literature (e.g., Hildreth 1983). In particular Canny (1983) showed that the first order derivatives of a Gaussian function are quasi-optimal edge detectors. This means that the energy of the first-order polynomial coefficients can be used to efficiently discriminate edges from noise by means of a threshold operation based on the theory of hypothesis tests for binary-decision problems. This threshold is therefore, computed from the statistical properties of the thermal and photon noise in the image and its propagation through the first-order polynomial coefficients. The noise is considered signal-independent and modeled as stationary additive noise with a Gaussian probability density function (PDF) and zero mean. Based on the PDF of the first order energy E_1 in uniform regions

$$p(E_1) = \frac{1}{2\sigma^2} exp\left[-\frac{E_1}{2\sigma^2}\right] \quad , \qquad (20)$$

we fix the threshold according to the desired percentage of noise rejection. In the case of noise with different PDF, such as Poisson, etc., other expression for $p(E_1)$ will be found; however, the algorithm strategy will not change. For more details on this strategy, the reader can refer to Escalante & Martens (1992). Experience has shown that expert users prefer a threshold that reduces about 70% of the noise contained in the image. More severe noise rejection results in blurred images, while less noise rejection still leaves the uncertainity of contour detection. By means of this threshold operation the energy measure is turned into a control image that provides information regarding the position of relevant edges in the image.

4.2. Description of the Algorithm

Figure 4 is a flow diagram that shows the multiresolution noise-reduction scheme proposed in this paper. At each level of the pyramid the smoothed image of the preceding pyramid level is taken as the input. $L(x,y)$ is the input image while $\hat{L}(x,y)$ is the output image. Block A represents the forward polynomial transforms. Although it is not strictly necessary, the window functions at the different pyramid levels will be identical. A subsampling factor of 2 will most often be included at each level, so that the equivalent window size also increases by a factor of 2 for each successive level of the pyramid. Using the first order polynomial coefficients, we obtain an energy measure in the block E as a noisy information

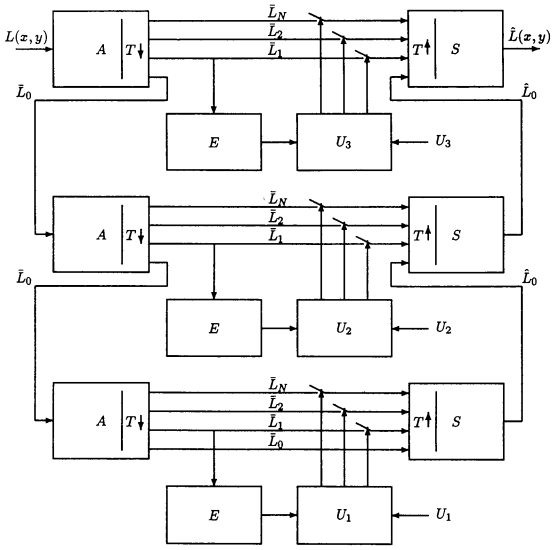

Fig. 4. The multiscale noise-reduction algorithm is presented, where $L(x,y)$ is the input image. Blocks A represent forward polynomial transforms followed by subsampling with a factor T. Blocks S represent inverse polynomial transforms preceded by upsampling with the same factor T. $\bar{L}_0$ are zero-order polynomial coefficients. Blocks E extract positions of contours from first-order polynomial coefficients. U_1, U_2 and U_3 are input thresholds. $\hat{L}(x,y)$ is the output image. Blocks U_i, $i = 1,2,3$, control reconstruction at each level of image resolution by opening or closing the switches.

source from which we have to decide whether the information observed corresponds to an image feature or to noise. This is achieved by means of the threshold operation described above.

The block S represents an adaptive inverse polynomial transform that reconstructs the astronomical image $\hat{L}(x,y)$ with noise reduction only in regions where edges were not detected (switches opened). As the image is subsampled by a factor of 2 at each pyramidal level, then the edges are analyzed at different spatial scales resulting in a multiresolution noise-reduction structure.

5. INTEGRAL PROCESSING SCHEME

As discussed in previous paragraphs, the polynomial transform is a mathematical model for image representation. One of its main characteristics is that it locally decomposes an image in terms of patterns that efficiently describe the different types of events that occur in an image. In this section we intend to show that this characteristic of the polynomial transform results in an general tool for different image processing applications. In the previous sections, we have shown how deconvolution and noise reduc-

tion can be achieved with the polynomial transform. We present in this section a scheme that integrates three different tasks: deconvolution, noise reduction and coding, these being some of the most important problems in image analysis.

All three applications have a common fundamental principle, i.e., signal must be discriminated from noise in order to restore, enhance and preserve only relevant image structures. As shown in the previous sections, the polynomial transform is an adequate tool for doing analysis as well as processing. We show in this section a possible scheme for implementing such a system. The adaptive algorithm for noise reduction presented in § 4 will be integrated to this system. Regarding the deblurring algorithm of § 3, it will also be included in the system but in an adaptive fashion, so that deblurring will only take place at positions where relevant information was found.

Relevant structure detection is achieved by means of an algorithm similar to that presented in § 3, i.e., by thresholding the energy of the first-order coefficients.

We generate a set of binary images indicating the positions of important intensity changes according to the respective spatial scale at each level in a pyramidal structure. All other positions of the image are assumed to contain only noise and can therefore, be represented with just the zero-order polynomial coefficients. Higher-order coefficients are set to zero in those positions. This operation implicitly reduces the noise in the image. Information entropy is therefore greatly reduced, i.e., significant compression rates can be obtained by quantizing these coefficients. The resynthesized image is reconstructed starting from the lowest resolution pyramidal level. Since high order coefficients were set to zero in noisy regions, deconvolution will only take place in regions where emission was detected. This operation is repeated at each pyramid level. In summary, the scheme proposes an algorithm that allows to adaptively process an image according to the scale-space representation of its luminance structures and noise. In Figure 5 we show a flow diagram with the proposed pyramidal scheme for integral processing. Blocks G_{σ_B} in Fig. 5 generate a Gaussian pyramid from the original image $L(x, y)$. Each block represents the convolution of the input image with a Gaussian function. After each block G_{σ_B} the image is subsampled. At each pyramidal level, meaningful image structures are detected by means of the blocks E_1. The original image is convolved with first-order derivatives of a Gaussian function whose spread is consistent with the resolution of the corresponding pyramid level. Afterwards, the energy of these images is computed. In the case of noisy images, this energy measures contributions from both signal and noise. Therefore, we threshold the energy in order to discriminate the location of intensity changes present

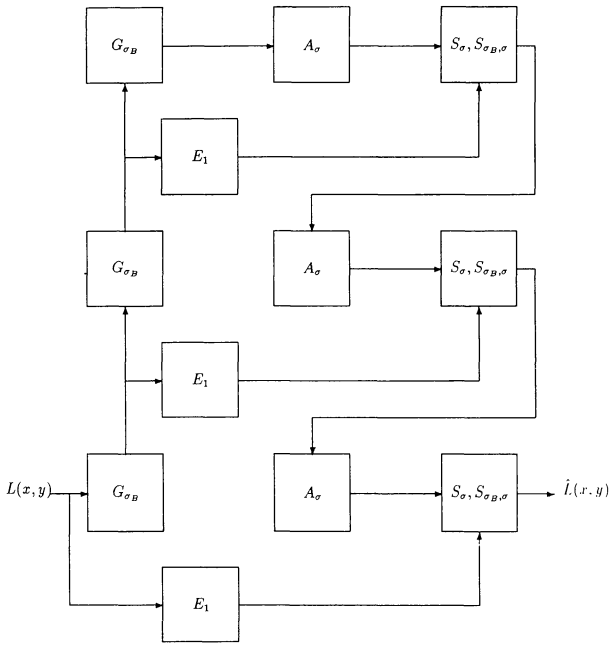

Fig. 5. The scheme of integral processing is shown for 3 levels, where $L(x, y)$ is input image. Blocks G_{σ_b} generate a gaussian pyramid. Blocks E_1 extract edge positions for different scales. Blocks A_σ represent forward polynomial transforms. Blocks $S_\sigma, S_{\sigma_B,\sigma}$ represent inverse polynomial transforms. Binary images given by blocks E_1 and the lowest the resolution image are sufficient to generate output image $\hat{L}(x, y)$.

in the image from noise contributions. This is done in a similar way to the procedure described in §4 in blocks E_1. The image at the top level is analyzed with a forward polynomial transform represented by the block A_σ. The regions where the thresholded energy image found relevant structures, pass through the block $S_{\sigma_B,\sigma}$, i.e., they are deconvolved in order to predict their representation at the higher next resolution level. The block $S_{\sigma_B,\sigma}$ consists of a modified inverse polynomial transform which considers both, the spread of the convolving Gaussian kernel σ_B and the spread of the Gaussian analysis window of the Hermite Transform σ. All other regions are restored to its original resolution level by means of the block S_σ. Steps 3 and 4 are repeated for each pyramidal level and the restored image $\hat{L}$ is obtained at the highest resolution level of the pyramid.

Noise reduction is achieved due to the fact that homogeneous regions without relevant structures are resynthesized at the lowest resolution level of the pyramid, while contours have been progressively deconvolved according to its scale-space representation (e.g., clouds and stars).

In order to efficiently code the image in a trans-

mission or storage system, the only necessary data to reconstruct the restored data are the image at the lowest resolution level of the Gaussian pyramid, and the energy images (binary images) generated by the block E_1 at each pyramid level. In this coding structure we code without preserving prediction errors. In this work the algorithm is designed specifically for astronomical images, that is, signals containing structures with a low frequency content (diffuse patterns) and high frequency content (stars) with noise; therefore, the prediction error images would mainly contain only noise information and very little structure. Neglecting these prediction errors does not cause visible effects.

6. IMAGE PROCESSING RESULTS

In this section we show results of the previously discussed image processing applications based on polynomial transforms in astronomical imagery.

To efficiently restore a noisy image, we need to discriminate image information from noise. In the case of astronomical images we find different types of structures (e.g., clouds and stars complexes) in the same image. In order to see how efficiently our method works, we have applied it to an optical image where weak structures are hardly detected due to the presence of noise. We have chosen the continuum-free Hα image of the galaxy NGC 3783. The image was obtained at the 2.12-m telescope in the Observatorio Astronómico Nacional at San Pedro Mártir, México with a CCD 1024×1024 pixel camera. (García-Barreto et al. 1996).

In Figure 6*a*, we present a raw CCD Hα image (NGC 3783). This image contains several diffuse patterns masked by noise. This noise is most likely of thermal origin or otherwise known as gaussian white noise. The signal-to-noise ratio (SNR), not including the nucleus, is about 0.98 dB. Including the nucleus, the SNR is 45.25 dB. This difference is due to the mean intensity values of the nucleus which are 2862 (arbitrary units), while the pixel mean values around the nucleus (on the ring) are 17. The noise standard deviation is 15. An astronomical study of nuclear region perhaps does not need any previous denoising process.

In Figure 6*b*, we present the Hα image of NGC 3783 restored by the polynomial-transform based method described in § 4. This image allows us to clearly detect the contours of a possible ring around the nucleus. In order to preserve high intensity changes such as the nucleus contour, the image was initially transformed by using a small size analysis window. On the other hand, regions outside the nucleus need to be severely smoothed in order to detect intensity changes. We used a four-level pyramidal structure in order to detect and restore low contrast, as well as high contrast structures in the image. The threshold parameters at each level of the pyramid selects the structures that are best detected and restored at every spatial scale.

TABLE 1

STATISTICS OF DIFFERENT NOISE REDUCTION ALGORITHMS

Image	Mean	Midpt	Stddev	Min	Max
6*a*	19.59	15.01	77.12	−5.542	2862
6*b*	19.59	13.20	76.99	1.506	2862
6*c*	18.41	15.01	54.59	12.19	1931
6*d*	19.80	13.25	77.09	1.506	2862

In Figure 6*c*, we show the Hα image of NGC 3783 restored by a 9×9 median filter. This filter is widely used in astronomical imaging; however, its ability to reject noise is limited as it can be seen from the figure. Furthermore, it introduces blocking effects in the image. This image processing was used by Forte et al. (1987) when showing the weak structure outside the nucleus.

Figure 6*d*, presents the restored Hα image of NGC 3783 using an adaptive filter based on the H-transform (Richter et al. 1991). It rejects the noise better than the median filter; however it seriously blurs the image.

Table 1 shows the statistics of images presented in Fig. 6 (object NGC3783 Hα); where Mean is the mean value of the pixel distribution, Midpt is the estimate of the median value of the pixel distribution, Stddev is the standard deviation of the pixel distribution, Min is the minimum pixel value, and Max is the maximum pixel value.

We note from Table 1 that in contrast to nonlinear filters (such as the median filter), adaptive linear filters, (such as those based on the polynomial-transform and the H-transform methods), produce images whose pixel mean, minimum, and maximum values do not deviate from their corresponding values in the original-image. This means that object's energy emission is preserved during the denoising process with adaptive linear filtering.

The image processed by the polynomial transform is sharper and shows galaxy structures that cannot be seen in any of the other images, including the original one, e.g., a bridge connecting the extremes of the ring across the nucleus in the E-W direction, almost perpendicular to the stellar bar. A study on 52 barred spiral galaxies processed with our algorithm appears in García-Barreto et al. (1996). Some evidence of the existence of these unveiled structures is also shown on that work.

Figure 7 shows the results of the integral processing scheme proposed in this paper. At the top-left the raw image (NGC3783Hα) is shown. Note that it is degraded by blur and noise. At the lower-left the

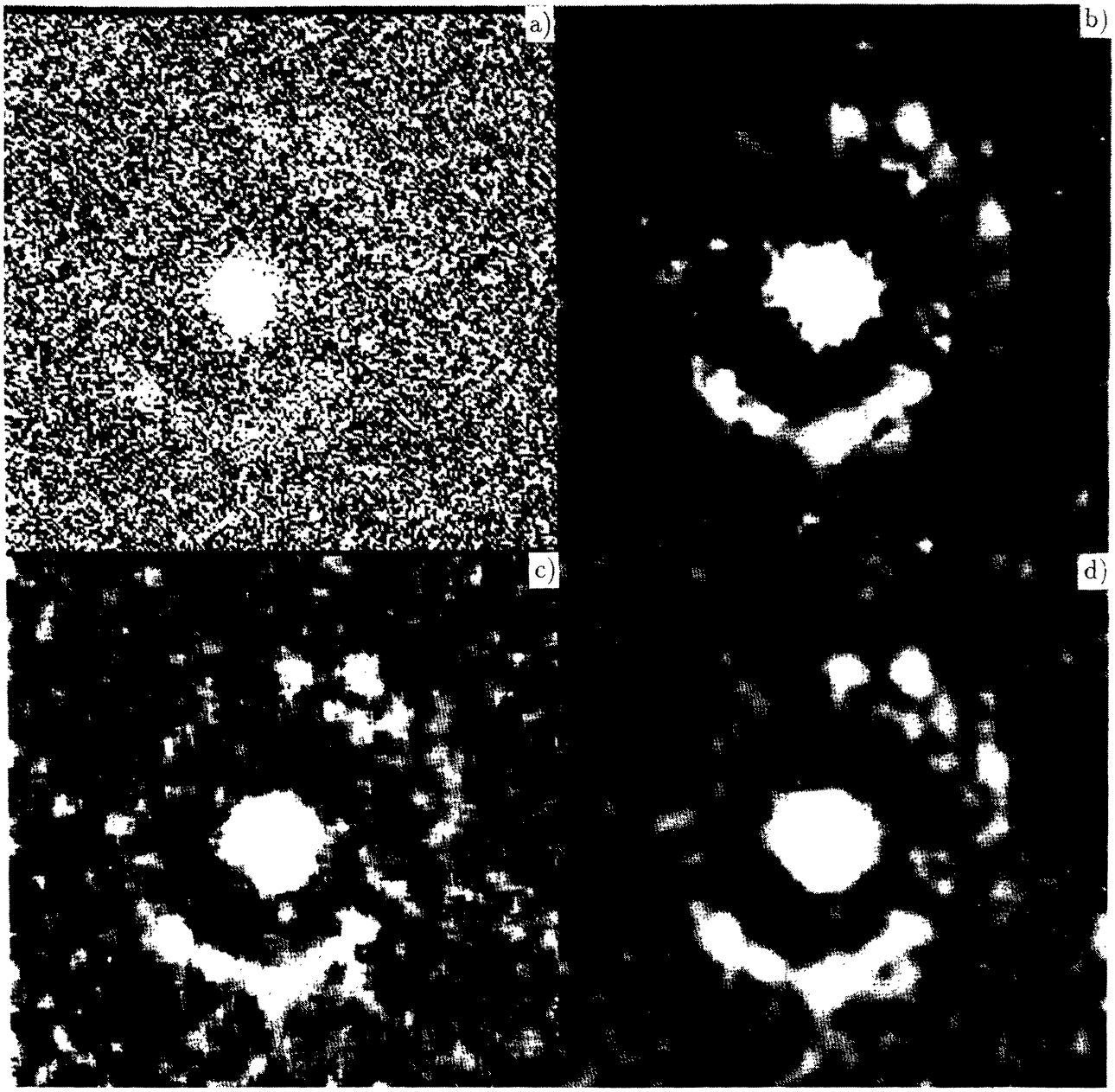

Fig. 6. Multiresolution noise reduction is presented. Where *a)* original image of the Hα continuum-free emission from the barred galaxy NGC 3783, *b)* image processed with noise-reduction algorithm by means of polynomial transform, *c)* image processed with median filter 9×9, and *d)* image processed with adaptive filter using local-to-noise ratio as a function of decreasing resolution (H-transform method).

multiresolution reconstruction process is depicted. It starts from lowest resolution level. Noise rejection and deblurring takes place only in positions selected by the binary images E1 generated at each pyramidal level. At the top-right the final reconstructed image is presented. A detail of this image can be appreciated at the lower-right. The coding scheme involved in this integral processing scheme (three pyramid levels) resulted in a compression rate of 60:1. No quantization stage was applied.

7. CONCLUSIONS

From the experimental results shown in the preceding section, we find strong evidence that multires-

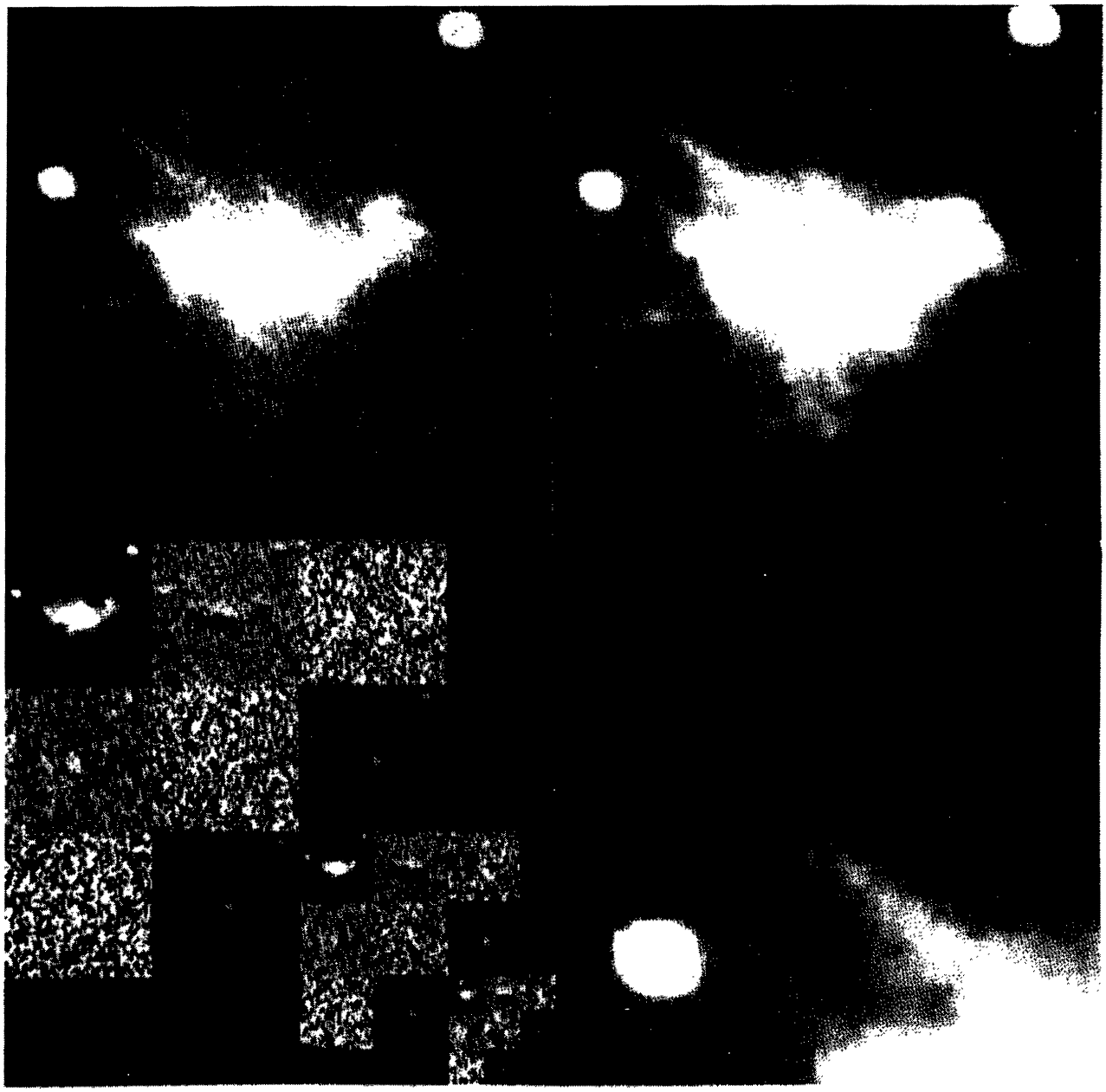

Fig. 7. The results of the integral processing scheme are shown. Top-left is original image, NGC 1275I (note that it is degraded by blur and noise). Lower-left is multiresolution image reconstruction starts from lowest resolution level. Noise rejection and deconvolution takes place only in positions selected by binary images E_1 at each pyramidal level. Top-right is reconstructed image. Lower-right is detail of reconstructed image. The coding scheme based on deconvolving compressed 60:1 for three pyramid levels. No quantization was applied.

olution methods represent an efficient alternative to process astronomical images. Many of these methods share similar basic principles such as adaptive filtering driven by the local image content. This is the case of several methods based on the H-transform, the wavelet transform (Mallat & Hwang 1992) and the polynomial transform among others. These transforms map the image from the spatial domain to a different space defined by a specific set of basis functions. Transforms like the H-transform produce blocking effects. In order to overcome this limitation the resulting image has to be blurred, which

severely impairs the image quality. Other models, such as the wavelets, use basic functions that contain much ringing. The resulting expansion coefficients have a limited ability to detect and represent meaningful image patterns such as contours. Efforts to overcome this problem with wavelets have been attempted by defining simpler basic functions, such as first-order Gaussian derivatives (Mallat & Hwang 1992). However, due to the orthogonality condition of the wavelet transform, the process of inverting this particular wavelet transform, i.e., the recovery of the image from the coefficients results in an extremely complicated procedure. The polynomial transform provides an efficient representation image model whose basic functions are related to derivatives of a Gaussian function. These operators are quasi-optimal contour detectors (Canny 1983). Furthermore, the inverse transform is not ill-posed and consists of simple interpolations.

In the case of image restoration from noise, the polynomial transform showed that the noise can be almost entirely suppressed while sharpness is preserved in important image features. This behavior is very different from traditional linear methods, because they achieve noise suppression only by broadening features significantly.

The multiscale feature of the algorithm allows to analyze an astronomical image at several resolutions in order to adapt the smoothing process to the position and contrast of contours. This characteristic allows us to include adaptive deconvolution in the same scheme. Deconvolution will take place only in the regions of the image where significant structures were located at each spatial scale. The result is an image with different degrees of deconvolution and noise reduction, i.e., in image locations where only noise was detected, smoothing occurred at all resolutions while deconvolution at none; where low contrast features were located, deconvolution took place at low resolutions and noise reduction at high resolutions, and in positions where high contrast features were detected deconvolution took place at all resolutions.

In the proposed pyramidal scheme for integral image processing, an image prediction from its lower resolution version takes place at each level of the pyramid. The prediction error consists mainly of noise information. Most of this information must be discarded, leading not only to noise rejection but also to image compression. This compression algorithm is especially useful for images with low SNR, such as astronomical images of faint objects.

This work was partially supported by UNAM grant DGAPA IN501095.

REFERENCES

Bijaoui, A., & Rué, F. 1995, Signal Processing, 46, 345
Burt, P., & Adelson, E. 1983, IEEE Comm-31, 532
Canny, J. F. 1983, MIT Artificial Intelligence Laboratory Technical Report AI-TR-720 (Boston: MIT)
_____. 1986, IEEE Trans. Pattern Anal. Mach. Intell, 8, 679
Carrillo, R. 1995, private communication
Escalante, R. B., & Martens, J. B. 1992, Journal of Visual Communication and Image Representation, 3, 272
Forte, J. C., Vega, E. I., Calderon, J. H., & Feinstein, C. 1987, AJ, 92, 301
García-Barreto, J. A, Franco, J., Carrillo, R., Venegas, M. S., & Escalante, R. B. 1996, RevMexAA, 32, 89
Haar, A. 1910, Math Ann., 69, 331
Hildreth, E. C. 1983, Comput. Vision Graphics Image Process., 22, 27
Kayargadde, V., & Martens, J. B. 1994, Comput. Vision Graphics Image Process, 56, 442
Koenderink, J. 1984, Biological Cybernetics, 50, 363
Mallat, S. G., & Hwang, W. L. 1992, IEEE Trans. on Inf. Theory. 38, 617
Martens, J. B. 1990, IEEE Trans. on Acoustics, Speech, and Signal Processing 38, 1595
Richter, G. M., Böhm, P., Lorenz, H., Priebe, A., & Capaccioli, M. 1991, Astron. Nach., 312, 345
Starck, J. L., Murtagh, F., & Bijaoui, A. 1995, in ASP Conf. Ser. Vol. 77, Astronomical Data Analysis Software and Systems IV, ed. R. A. Shaw, H. E. Payne, & J. J. E. Hayes (San Francisco: ASP), 279
Starck, J. L., Murtagh, F., Pirenne, B., & Albrecht, M. 1996, PASP, submitted
Szegö, G. 1959, in Orthogonal Polynomials, Coiloquium Publications, (New York: Am. Math. Soc.), Vol. XXIII
Venegas, M. S., Escalante, R. B., García, U. F., & García, B. J. A. 1995, Applications of Digital Image Processing XVIII 2564, ed. A. G. Tescher (San Diego: SPIE), 136
Young, R. 1985, General Motors Research Technical Report GMR-4920, (Detroit: General Motors)

Boris Escalante-Ramírez and Santiago Venegas-Martínez: División de Estudios de Posgrado, Facultad de Ingeniería, UNAM, Apartado Postal 70-256, 04510 México, D.F., México (boris@verona.fi-p.unam.mx.
José A. García-Barreto: Instituto de Astronomía, UNAM, Apartado Postal 70-264, 04510 México, D.F., México (tony@astroscu.unam.mx).